Range Measurements of Fission Products. I. Comparison with Stopping Theory*

Miles Pickering and John M. Alexander
Department of Chemistry, State University of New York, Stony Brook, New York 11790
(Received 6 December 1971)

Range distributions in H_2, He, Ne, and Ar, are reported for seven fission products (Zr^{97}, Mo^{99}, Rh^{105}, Pd^{112}, In^{115}, Te^{132}, Ce^{143}). The method of electrostatic collection of these products has been explored, and high collection efficiencies are observed for most products. The width of the observed distributions is resolved into a contribution from the stopping effects and a contribution from the fission process. The average range values and the stopping straggling are compared with the theory of Lindhard, Scharff, and Schiøtt. The differences between theory and experiment are ≈5 to 50%.

I. INTRODUCTION

This is the first of two papers on the stopping of fission fragments in gases.[1] Radiochemical methods were used to measure the average ranges and distributions in range ("range straggling") for the recoiling fission fragments produced by Cf^{252}. Previous work of this type has been done by a stacked-foil method[2-11]; but the results are always complicated by the range straggling created by stopper inhomogeneities. Range distribution measurements in gases should give range straggling values that result from only two effects, the broadening of the distribution by the statistical effects inherent in the stopping process and the variation of initial fragment energy. These two effects have been separated, and the latter will be the subject of the accompanying paper.[1]

A variety of fission products was observed in several stopping media. The recoils were collected electrostatically,[12-16] and various tests of method implied that the spatial distributions of the collected products were primarily due to the range distributions rather than other causes. The variation of the observed straggling with the mass of stopping gas allowed the separation of fission-produced straggling and stopping-produced straggling.

We have compared our measured values of the straggling from the stopping process (ρ_s) with the predictions of the stopping theory of Lindhard, Scharff, and Schiøtt (LSS),[17] an *a priori* theory based on the Thomas-Fermi potential. The electronic stopping parameter, k, has been fixed by the measured values of the average range. The comparison of LSS theory with the measurements shows the observed straggling parameters to be about 35% greater than predicted.

II. EXPERIMENTAL MEASUREMENTS AND CORRECTIONS

A. Experimental Procedures

Measurements were made by stopping products from the spontaneous fission of Cf^{252} in gases, electrostatically collecting them on a charged plate,[12-16] and determining the intensity of individual γ rays from different sections of the plate. The spatial distribution of radioactivity on the plate was then related to the desired mean and variance of the range distribution in the stopping gas.

The experimental apparatus consisted of three basic parts: a fission-fragment source (Cf^{252}), a collimator, and a gas-filled chamber with charged plates for electrostatic collection. Figure 1 shows a schematic diagram.

The source of Cf^{252} deposited by self-transfer onto a tantalum disk gave $\approx 2\times10^7$ fissions/min. It was covered with a thin (20-μin.) Ni window to prevent self-transfer of the Cf^{252}. The correction for the effect of the thickness of the cover foil was determined both for the mean range and the range straggling.

The collimator accepted fragments emitted in a cone of 12.4° apex angle. This collimation defined an axis along which the ranges were measured. There is a slight foreshortening of the observed ranges and a broadening of the range distribution due to the width of this cone. This has been corrected for as described later.

The collection chamber was a gas-filled volume with two charged plates covered by aluminum foil. A large fraction of the fragments was collected on the plates by the horizontal electrostatic field. Potentials of up to 1000 V were applied to the plates, and smaller potentials to several additional elec-

trodes to reduce effects of the fringing field. The chamber was aluminum throughout; hence it formed a Faraday cage, and prevented the penetration of external electrostatic fields. Field strengths ranged up to 53 V/cm.

In a typical experiment the chamber was evacuated by a mechanical pump to a pressure of 1–3 $\times 10^{-3}$ mm Hg and maintained at this pressure overnight. High-purity gases were used, and the chamber was always flushed with the gas to be used at least three times before the final filling. Gas pressures ranged from 0.25 to 0.04 atm, and were measured by a mercury manometer.

A typical exposure lasted three days. At the end of this time, the plates were removed and sprayed with lacquer to prevent accidental mechanical transfer of activity. Then the foils were cut into strips and folded to form convenient samples for γ-ray counting. The γ rays from each sample were counted repeatedly over a period of a few days with a Ge(Li) γ-ray detector and pulse-height analyzer system. The data were transmitted from the analyzer memory through an interface to an IBM 1800 computer which integrated the peaks in the γ-ray spectrum and subtracted an appropriate background. A decay curve was fitted by least squares to the data for each isotope in each sample. Each data point was weighted by the square root of the number of counts.

From the measured activity at each distance along the plate, a differential-range histogram was drawn for each observed product. Figure 2 shows a typical range histogram. This histogram displays noticeable negative skewness which is believed to be of instrumental origin. We believe that fission fragments have traversed somewhat different path lengths before entering the gas, because of the diffusion of the Cf into its backing or the accumulation of foreign matter on the source layer. A Gaussian curve was fitted to the data points on the peak and on the long-range side of the peak. The mean range and the standard deviation were taken directly from the fitted curve. Both were then multiplied by the gas density to convert to units of mg/cm^2. These interim values were corrected as described in the next section.

A test of this fitting procedure was performed by computing the root-mean-square deviation of the observed range distribution including skewness. In no case was this raw width greater than 140% of the fitted width, in most cases $\approx$120%. This test was performed on the product Pd^{112}, since the peak-to-background ratio for its γ ray was most favorable. The error in the straggling parameter introduced by fitting the Gaussian distribution is expected to be less than $\approx$20% of the total correction of 20–40%, or 4–8%.

There are at least two assumptions underlying this whole procedure. One is that the actual range distribution is represented by a Gaussian, that is, that an infinitely thin fission source would give such a distribution. The second is that there are no interfering, unresolved γ rays in any of the peaks. The first assumption is based on the corresponding property of "thin" sources of α radioactivity, and should extend to all sources of heavy ions. The assumed purity of the γ peaks is based on the observed decay rate as well as the agreement in energy. A special experiment (described in Sec. III) was performed in order to assign γ rays to individual fission products. The measurement of the intensities, energies, and approxi-

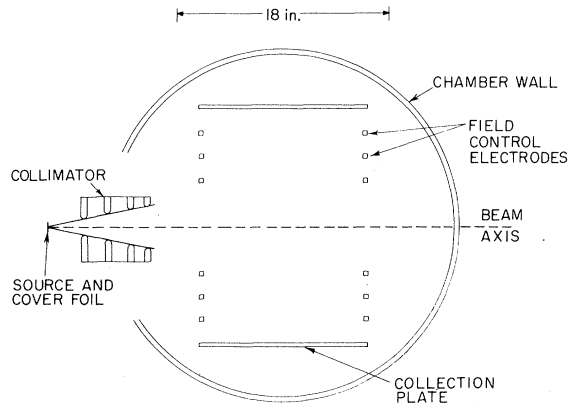

FIG. 1. Schematic diagram of the collection chamber. Recoil ions from the source were collimated and stopped in the gas-filled region, then electrostatically collected on the plates. The field control electrodes minimized fringing of the field.

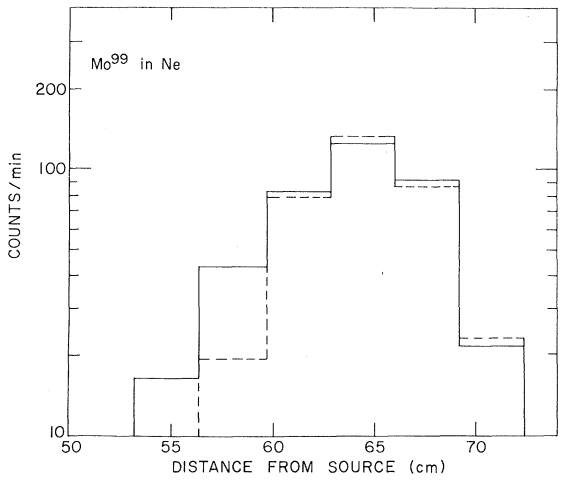

FIG. 2. A sample differential-range histogram and the fitted Gaussian distribution. The solid lines are the measured results and the dashed line is the fitted curve.

TABLE I. Properties of the observed nuclides.

Observed product	γ energy (keV)	Half-life $t_{1/2}$
Zr^{97}	665 (Nb^{97})	17.0 h
Mo^{99}	140	67 h
Rh^{105}	306	36 h
Rh^{105}	319	36 h
Pd^{112}	617 (Ag^{112})	21 h
Cd^{115}	335 (In^{115m})	53.5 h
I^{131}	364	8.05 day
Te^{132}	230	77 h
I^{133}	530	20 h
Xe^{135}	250	9.2 day
Ce^{141}	145	32.5 day
Ce^{143}	293	34 h
Sm^{153}	103	47 h

mate half-lives, usually sufficed for identification of the various products. Fission yields[18] and γ-ray abundances[19] from the literature were also used as a cross-check. The observed products, their half-lives and the observed γ rays are summarized in Table I.

The intensities of all the peaks cited in Table I were strong in the calibration experiment. However, in the electrostatic collection experiments only peaks from Zr^{97}, Mo^{99}, Rh^{105}(319 keV), Pd^{112}, Cd^{115}, Te^{132}, and Ce^{143} were strong enough to measure differential-range curves. The other peaks (Rh^{105} at 306 keV, I^{131}, I^{133}, Xe^{135}) were too weak to allow any other measurement than the collection efficiency. Finally, the 104-keV peak of Sm^{153} was weak and suffered from a high background. Because of the uncertainty about it, values based on this observation are not given much weight.

B. Corrections to the Mean Range Values

1. Correction for the cover foil. In one experiment a foil similar to the one used as a cover foil for the Cf^{252} source was placed in the collimator section. An average range determination was made in H_2 after penetration through the two Ni foils.

We use $\bar{R}_N$ to denote the observed average range with only the one Ni cover foil and $\bar{R}_{NN}$ to denote the observed average range with the two Ni foils. Then the difference δR given by

$$\delta R = \bar{R}_N - \bar{R}_{NN} \tag{1}$$

gives the effect of degradation in one Ni foil, since energy loss is linear with thickness in this energy region. The results of this experiment are given in Table II. We see that $\delta R/\bar{R}_N$ is very nearly constant at 12%. Hence, range values obtained with only the one cover foil were multiplied by the constant factor $1+(\delta\bar{R}/\bar{R}_N)\equiv 1.12$ to correct for the Ni cover foil. The range straggling was not affected appreciably by the presence of the Ni foil and therefore no correction was required. This observation is consistent with the expectation that most range straggling occurs near the end of the range.

2. Correction for geometry. The collimator did not produce an absolutely parallel beam, but one with a maximum divergence of 12.4°. This means that the apparent range was slightly less than the true range (foreshortening). If the true range is R_t, the projected range in the beam direction is $R_{\text{proj}} \equiv R_t \cos\theta$ for any angle θ.

Since the distribution of recoil angles is proportional to $\sin\theta$ the average projected range $\bar{R}_{\text{proj}}$ is

TABLE II. Measurements of the effect of a Ni cover foil.

Observed product	Average range with one Ni foil [a] $\bar{R}_N$ (mg/cm^2 H_2)	Average range with two Ni foils [a] $\bar{R}_{NN}$ (mg/cm^2 H_2)	δR	$\frac{\delta R}{\bar{R}_N}$	$\bar{\rho}_N$ [b]	$\bar{\rho}_{NN}$ [c]
Zr^{97}	0.817	0.722	0.095	0.116	0.0519	0.0383
Mo^{99}	0.818	0.711	0.107	0.13	0.0403	0.0385
Rh^{105}	0.804	0.695	0.109	0.136	0.0408	0.0421
Pd^{112}	0.775	0.674	0.101	0.130	0.0396	0.0423
Cd^{115}	0.763	0.672	0.091	0.119	0.0402	0.0470
Te^{132}	0.754	0.688	0.066	0.088	0.0395	0.0378
Ce^{143}	0.702	0.623	0.079	0.112	0.0369	0.0446
Average				0.119	0.0413	0.0415

[a] $\bar{R}_N$ is the average projected range uncorrected for geometry and the single Ni cover foil. $\bar{R}_{NN}$ is the corresponding quantity observed with two Ni cover foils.

[b] $\bar{\rho}_N$ is the observed standard deviation divided by $\bar{R}_N$, uncorrected.

[c] $\bar{\rho}_{NN}$ is the observed standard deviation divided by $1.12\bar{R}_{NN}$, uncorrected.

given by

$$\bar{R}_{\text{proj}} = \frac{\int_0^{\theta_{\max}} R_t \cos\theta \sin\theta d\theta}{\int_0^{\theta_{\max}} \sin\theta d\theta} \tag{2}$$

and

$$\bar{R}_{\text{proj}} = \frac{R_t \sin^2\theta_{\max}}{2(1-\cos\theta_{\max})} = \alpha R_t , \tag{3}$$

where

$$\alpha = \frac{\sin^2\theta_{\max}}{2(1-\cos\theta_{\max})} = 0.9882 . \tag{4}$$

This correction is only slightly more than 1%, and is very well known. The final corrected average range, incorporating both geometry and foil corrections is denoted by $\langle R\rangle$, where

$$\langle R\rangle = 1.12\bar{R}_{\text{proj}}/\alpha , \tag{5}$$

where $\bar{R}_{\text{proj}}$ is the uncorrected average range as determined in the experiment.

C. Corrections to Range Straggling Values

For a Gaussian range distribution $P(R)dR$ we have an average range $\bar{R}$ with standard deviation σ; the straggling parameter ρ is given by

$$\rho = \sigma/\bar{R} , \tag{6}$$

where $\bar{R}$ and σ are in the same units. All the observed and calculated distributions have been approximated by the Gaussian distribution, and the property of variance additivity has been used to correct the observed standard deviations for diffusion, width of sample, and geometry.

1. Correction for diffusion. From the theory of aerosols[20] it is known that the average drift velocity $\bar{v}$ in an electric field is given by

$$\bar{v} = De\bar{E}/kT , \tag{7}$$

where D is the diffusion coefficient, $\bar{E}$ is the field strength, e is the electronic charge, k the Boltzmann constant, and T the absolute temperature.[21]

It is also known [22] that

$$\sigma^2_{\text{diff}} = 4Dt , \tag{8}$$

where σ^2_{diff} is the diffusion-produced variance, and t is the duration of diffusion (from the time of thermalization of the ion to its collection on the plate).

Since

$$d \approx \bar{v}t , \tag{9}$$

where d is the distance to the plate from the beam axis, then

$$t = d/\bar{v} = dkT/De\bar{E} , \tag{10}$$

and

$$\sigma^2_{\text{diff}} = 4D\frac{dkT}{De\bar{E}} = \frac{4dkT}{e\bar{E}} . \tag{11}$$

The value of σ^2_{diff} is about 1% of the total variance for all experiments except those in Ne; for Ne a slightly lower field strength was used and $\sigma^2_{\text{diff}}/\sigma^2$ was about 2.3%.

2. Sheppard correction. A correction is required for the fact that the collection strips had finite width.[23] If h is the width (in units of mg/cm^2) of the samples, a correction of $h^2/12$ (called the Sheppard correction) must be subtracted from the observed variance σ^2. This correction reduced the values of σ and ρ by 7 to 12%.

3. Correction for geometry. In Sec. B 2 it was shown that the average projected range $\bar{R}_{\text{proj}}$ is related to the average true range R_t by $\alpha R_t = \bar{R}_{\text{proj}}$, where

$$\alpha = \frac{\sin^2\theta_{\max}}{2(1-\cos\theta_{\max})} . \tag{12}$$

The variance σ^2_{geom} of the projected distribution due only to geometry is given by

$$\sigma^2_{\text{geom}} = \frac{\int_0^{\theta_{\max}} (\alpha R_t - R_t\cos\theta)^2 \sin\theta d\theta}{\int_0^{\theta_{\max}} \sin\theta d\theta} \tag{13}$$

and

$$\sigma^2_{\text{geom}} = \frac{R_t^2}{3(1-\cos\theta_{\max})}\left[(\alpha-\cos\theta_{\max})^3 - (\alpha-1)^3\right], \tag{14}$$

since

$$\rho^2_{\text{geom}} = \frac{\sigma^2_{\text{geom}}}{\bar{R}^2_{\text{proj}}} = \frac{\sigma^2_{\text{geom}}}{\alpha^2 R_t^2} , \tag{15}$$

$$\rho^2_{\text{geom}} = \frac{1}{3\alpha^2(1-\cos\theta_{\max})}\left[(\alpha-\cos\theta_{\max})^3 - (\alpha-1)^3\right]$$

$$= 0.000\,47 . \tag{16}$$

This correction reduced the values of σ and ρ by about 3%.

Hence the corrected variance in range σ^2_{corr} is

$$\sigma^2_{\text{corr}} = \sigma^2_N - \sigma^2_{\text{diff}} - \sigma^2_{\text{geom}} - h^2/12 \tag{17}$$

and

$$\rho^2_{\text{corr}} = \sigma^2_{\text{corr}}/\langle R\rangle^2 . \tag{18}$$

The values of σ^2_{corr} and ρ^2_{corr} contain both the effect of the statistical nature of the stopping process σ^2_s and the initial energy distribution of the fission process σ^2_f ($\sigma^2_{\text{corr}} = \sigma^2_s + \sigma^2_f$).

The corrected values for both mean ranges and

straggling parameters are summarized in Table III. The discussion of these values and the separation of the stopping and fission effects is given in Sec. IV.

4. Systematic errors in the analysis. The data analysis just described is subject to various sources of systematic error. First, the assumption has been made that the range distribution should be represented by a Gaussian form. The deviation of the observed distribution from this form has been attributed to source thickness and has been eliminated by fitting to a Gaussian, as discussed in Sec. A. Secondly, variance additivity has been assumed for all sources that contribute to the width of the distribution. This assumption is not clearly justifiable for the geometrical broadening. But since the maximum range broadening due to this effect is very small $[(1-\cos\theta_{\max})\langle R\rangle$ or $0.023\langle R\rangle]$, the correction to σ from this effect is not serious. A more precise method would give a somewhat larger correction, but still much less than other uncertainties. Thus, there are two corrections that introduce systematic errors: (a) the effect of the source that may have been overestimated and (b) the effect of geometry that may have been underestimated.

5. Comparison with previous measurements. One can compare the values of the straggling parameters with those of previous workers. To make this comparison the values of ρ_{corr} have been grouped as follows: "light" fragments (97–99), "intermediate" fragments (105, 112, 115), and "heavy" fragments (132–143). A similar grouping has been made for the data of Petrzhak,[6] Katcoff, Miskel, and Stanley,[2] Marsh and Miskel,[3] Aras, Menon, and Gordon,[9] and Cumming and Crespo.[10] Figure 3 shows the values of ρ for these groups. Katcoff, Miskel, and Stanley,[2] and Marsh and Miskel[3] report values which are very close to those of this work. Aras, Menon, and Gordon[9] report values about twice as large as those reported here. The values of Aras, Menon, and Gordon[9] were obtained with Al leaf as a stopper and may suffer from foil inhomogeneities. In all cases Petrzhak and co-workers[6] report values for the straggling parameter that are 25–40% smaller than those in the present work. It is difficult to understand these low straggling parameters unless the energy distributions in the fission of U^{233} are considerably smaller than for Cf^{252}. It is likely that there is some systematic error either in the present work or in that of Petrzhak and co-workers.[6] This apparent discrepancy has not been resolved.

III. COLLECTION EFFICIENCY

The experimental method used in this work depends on the retention of an ionic charge by the fragments emitted from the source. This charge must be retained, even after the ions have been slowed to thermal velocities. If the fragment remains ionized, then the electric field will attract

TABLE III. Experimental results. Experimental values of the average range $\langle R\rangle$, and the straggling parameter ρ_{corr} in various gases.

Observed product	H_2	He	Ne	Ar
		$\langle R\rangle$ (mg/cm^2)		
Zr^{97}	0.941 ± 0.011 [a] (2) [b]	2.892 ± 0.02 (2)	4.963 ± 0.002 (2)	4.83 ± 0.15 (2)
Mo^{99}	0.945 ± 0.017 (2)	2.877 ± 0.02 (2)	4.939 ± 0.001 (2)	4.81 ± 0.16 (2)
Rh^{105}	0.925 ± 0.015 (2)	2.782 ± 0.02 (2)	4.832 ± 0.009 (2)	4.56 ± 0.14 (3)
Pd^{112}	0.893 ± 0.008 (3)	2.700 ± 0.025 (2)	4.624 ± 0.009 (2)	4.39 ± 0.17 (2)
Cd^{115}	0.888 ± 0.009 (3)	2.688 ± 0.02 (2)	4.519 ± 0.03 (2)	4.36 ± 0.16 (2)
Te^{132}	0.870 ± 0.006 (3)	2.625 ± 0.03 (3)	4.24 ± 0.07 (3)	4.13 ± 0.14 (2)
Ce^{143}	0.808 ± 0.011 (2)	2.370 ± 0.015 (2)	3.78 ± 0.08 (3)	3.71 ± 0.10 (2)
Sm^{153}	0.785 ± 0.013 (2)	2.313 (1)	3.56 ± 0.09 (3)	3.51 ± 0.11 (2)
		ρ_{corr}		
Zr^{97}	0.047 ± 0.002 [a] (2) [b]	0.038 ± 0.005 (2)	0.046 ± 0.001 (2)	0.060 ± 0.001 (2)
Mo^{99}	0.036 ± 0.002 (2)	0.036 ± 0.002 (2)	0.0452 ± 0.0001 (2)	0.056 ± 0.007 (2)
Rh^{105}	0.037 ± 0.003 (2)	0.043 ± 0.001 (2)	0.0492 ± 0.0002 (2)	0.052 ± 0.008 (3)
Pd^{112}	0.036 ± 0.005 (3)	0.039 ± 0.002 (2)	0.048 ± 0.0004 (2)	0.056 ± 0.003 (2)
Cd^{115}	0.036 ± 0.001 (3)	0.043 ± 0.001 (2)	0.064 ± 0.002 (2)	0.063 ± 0.010 (2)
Te^{132}	0.035 ± 0.003 (3)	0.041 ± 0.004 (3)	0.056 ± 0.002 (3)	0.064 ± 0.007 (2)
Ce^{143}	0.033 ± 0.006 (2)	0.038 ± 0.001 (2)	0.050 ± 0.007 (3)	0.077 ± 0.009 (2)

[a] Quoted uncertainties are average deviations from the mean.
[b] In parentheses is indicated the number of determinations.

it to the plate so rapidly that diffusion processes will not have time to broaden or distort the projected range distribution appreciably. If the fragment is neutralized, however, the field will have no effect, and the fragments on the plates will have arrived by random paths, under the influence of diffusion. The question of whether the fragments remain charged can most easily be answered by measuring the collection efficiency on each plate in experiments with an electric field, and with no field.

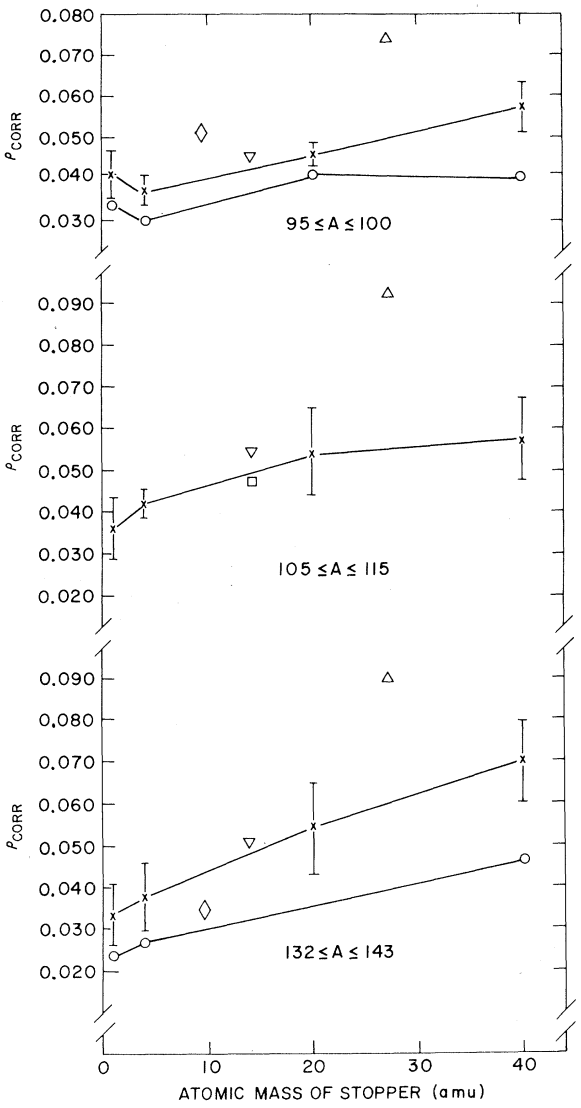

FIG. 3. Corrected straggling parameter vs mass of stopper for three groups of fission products: ×, data from the present work; ▽, data from Katcoff, Miskel, and Stanley, Ref. 2; △, data from Aras and co-workers, Ref. 9; □, data from Marsh and Miskel, Ref. 3; ◇, data from Cumming and Crespo, Ref. 10; ○, data from Petrzhak, Ref. 6.

As described in the previous section, a measurement was made of the saturation intensity of each γ ray. For this measurement a foil was placed over the aperture of the collimator, and all the emerging fragments were embedded in this catcher. The saturation radioactivity was also measured for all products in the electrostatic collection experiments. The ratio of these saturation activities (corrected for the decay of the Cf^{252} source) is the fraction of fragments collected, or the "collection efficiency."

The numerical values of the measured collection efficiencies are given in Table IV. The results can be summarized as follows: (1) Collection is reproducible to about ±10% from experiment to experiment, and there is only a slight dependence on the nature of the collection gas; (2) no collection (<2%) is observed on the positive plate; (3) collection is greatly reduced if the field is turned off (<4% on each plate); (4) for certain species, Te, I, and Xe, the collection efficiency is very low, but for most products it is about 0.8–0.9.

The observations above suggest that most of the fragments remain charged. The reduction of collection efficiency when the field is turned off, and the selective collection on the negative plate support this view. The observation of zero collection efficiency on the positive plate is in sharp contrast to the observations of previous workers. In three separate projects that used electrostatic collection of accelerator-produced radioactive products,[13-16] significant amounts of activity were observed on the positive plate. However, in all these experiments the accelerator beam passed through the collection region, and the observed effect may have been produced by the plasma that the beam created.

All radioactive products observed in this experiment are the daughters of primary fission products far from β stability (hence short-lived). This primary distribution of charge has been studied in detail for neutron-induced fission of U^{235} and a tabulation of the values of the most probable charge Z_p has been made by Wahl and co-workers.[24] There is not much information on other fissionable nuclei, but Coryell, Kaplan, and Fink[25] have proposed a simple means of estimating the most probable charge $Z_p(A_c)$ by reference to the values for U^{235}. Their method is to add a small correction ΔZ_p to the Z_p for U^{235},

$$Z_p(A_c) = Z_p(U^{235}) + \Delta Z_p(A_c), \tag{19}$$

$$\Delta Z_p(A) = \tfrac{1}{2}(Z_c - 92) - 0.19(A_c - 236) + 0.19(\nu_t - 2.5), \tag{20}$$

where Z_c is the charge of the fissioning nuclide

TABLE IV. Average collection efficiency.

Observed product	Stopping gas: Argon [a]	Helium [b]	Neon [c]	Hydrogen [d]
Zr^{97}	0.79±0.04 [e]	0.88±0.08 [e]	0.86±0.07 [e]	0.87±0.06
Mo^{99}	0.77±0.01	0.89±0.08	0.83±0.03	0.89±0.06
Rh^{105}(306 keV)	0.78±0.02	1.02±0.02	0.86±0.01	0.95±0.02
Rh^{105}(319 keV)	0.75±0.06	0.86±0.09	0.85±0.01	0.88±0.04
Pd^{112}	0.77±0.05	0.91±0.02	0.80±0.05	0.96±0.04
Cd^{115}	0.69±0.05	0.85±0.02	0.73±0.04	0.87±0.13
I^{131}	0.36±0.02	0.43±0.02	0.38±0.02	0.53±0.03
Te^{132}	0.35±0.02	0.48±0.02	0.49±0.04	0.44±0.03
I^{133}	0.12±0.01	0.13±0.03	0.16±0.02	0.11±0.01
Xe^{135}	<0.02	<0.02	<0.02	<0.02
Ce^{141}	0.8 ±0.2	0.93±0.02	0.74±0.04	0.80±0.08
Ce^{143}	0.82±0.04	0.94±0.03	0.82±0.02	0.96±0.08
Sm^{153}	0.57±0.07	0.73	0.64±0.01	0.79±0.10
Average	0.63	0.75	0.68	0.75
Pressure (atm)	0.03–0.05	0.21–0.28	0.07–0.09	0.19–0.14

[a] The average of three experiments with field strength of 0.137 abvolt/cm (41 V/cm).
[b] The average of three experiments with field strength of 0.175 abvolt/cm (53 V/cm).
[c] The average of three experiments with field strength of 0.066 abvolt/cm (20 V/cm).
[d] The average of three experiments with field strength of 0.175 abvolt/cm (53 V/cm).
[e] The quoted uncertainties are average deviations.

and A_c its mass, and ν_t is the total number of neutrons emitted. There is close agreement between our calculated values of Z_p and those interpolated from the recent experimental data of Chiefetz *et al.*[26] With these equations and the Wahl charge dispersion curve for U^{235},[24] the primary yields have been obtained for each nuclide in the observed mass chains. Table V gives a list of these estimated yields along with the collection efficiencies observed in H_2.

For all primary products except those in the mass chains 131, 132, 133, and 135, the collection efficiency is high (≈90%) for all major products (Sr, Y, Zr, Nb, Mo, Tc, Ru, Rh, Pd, Ag, Cs, Ba, La). Since there is no collection in the 135 mass chain, Te, I, and Xe have not been collected. From the 11% efficiency for collection for I^{133} one can infer that Sb must collect at least partially (≈30%). To account for the collection in the 132, and 131 chains, collection efficiency must be quite high for Sn.

In the present work no attempt was made to study the mechanism of the collection process in detail because so many products were satisfactor-

TABLE V. Estimated primary product yields compared with the collection efficiency in H_2.

Observed product	Z_p	Primary yields (%)			Collection efficiency in H_2 (%)
Zr^{97}	39.07	Sr^{97} (18)	Y^{97} (56)	Zr^{97} (24)	87
Mo^{99}	39.85	Y^{99} (27)	Zr^{99} (55)	Nb^{99} (14)	89
Rh^{105}	42.07	Nb^{105} (18)	Mo^{105} (56)	Tc^{105} (24)	92
Pd^{112}	44.89	Ru^{112} (24)	Rh^{112} (56)	Pd^{112} (18)	96
Cd^{115}	45.85	Rh^{115} (27)	Pd^{115} (55)	Ag^{115} (14)	87
I^{131}	50.99	Sn^{131} (20)	Sb^{131} (58)	Te^{131} (20)	53
Te^{132}	51.40	Sn^{132} (9)	Sb^{132} (46)	Te^{132} (39)	44
I^{133}	51.84	Sb^{133} (27)	Te^{133} (55)	I^{133} (14)	11
Xe^{135}	52.75	Te^{135} (31)	I^{135} (53)	Xe^{135} (10)	<02
Ce^{141}	55.18	Xe^{141} (12)	Cs^{141} (55)	Ba^{141} (28)	80
Ce^{143}	55.97	Cs^{143} (21)	Ba^{143} (58)	La^{143} (19)	96
Sm^{153}	60.07	Pr^{153} (18)	Nd^{153} (56)	Pm^{153} (24)	79

ily collected. It is of primary importance simply that the collection efficiencies showed a reproducible pattern and that this pattern is consistent with a model of rapid collection by an electrostatic field. This implies that the distribution of radioactivity on the plate can be directly related to the distribution of projected ranges.

IV. COMPARISON OF THE OBSERVATIONS WITH STOPPING THEORY

This discussion concerns the way in which the effects of the stopping process can be disentangled from the effects of the fission process.

The stopping theory of LSS[17] is based on a statistical approach. It assumes that there are two sorts of completely uncorrelated processes producing the energy loss, a "nuclear" or ion-atom energy transfer, and an "electronic" or ion-electron energy transfer. Electronic stopping predominates at high energies, such as those of full-energy fission fragments, and nuclear or ion-atom stopping is important at low energies. In the LSS treatment, ranges and energies are transformed into the dimensionless variables ρ_L (not a straggling parameter) and ϵ, respectively, where

$$\rho_L = \pi a^2 N \gamma \langle R \rangle , \tag{21}$$

$$\epsilon = E \frac{a A_2}{Z_1 Z_2 e^2 (A_1 + A_2)} , \tag{22}$$

$\langle R \rangle$ and E are range and energy, A_1 and Z_1 are the mass and atomic number of the recoil, A_2 and Z_2 are the mass and atomic number of the stopping gas, N is the atomic density, and ϵ is the electronic charge. The parameter a is given by

$$a = 0.8853 a_0 (Z_1^{2/3} + Z_2^{2/3})^{-1/2} , \tag{23}$$

TABLE VI. Parameters leading to the trial values of the straggling from stopping effects.

Observed product	Stopping gas	ϵ	ρ_L	k_{emp}	$10^4(\rho_s^2)_{trial}$	$10^4\rho_{corr}^2$
Zr^{97}	H_2	249.8	126.2	0.22	0.38	21.90
Zr^{97}	He	473.8	348.8	0.12	0.91	14.28
Zr^{97}	Ne	368.3	361.8	0.10	4.80	21.34
Zr^{97}	Ar	327.7	225.7	0.145	6.65	35.40
Mo^{99}	H_2	237.8	122.5	0.22	0.36	13.17
Mo^{99}	He	451.4	336.0	0.12	0.95	13.17
Mo^{99}	Ne	352.3	351.4	0.10	4.98	20.43
Mo^{99}	Ar	314.4	220.6	0.145	6.73	27.45
Rh^{105}	H_2	208.5	109.7	0.22	0.43	13.54
Rh^{105}	He	396.8	298.6	0.12	1.10	18.74
Rh^{105}	Ne	313.2	322.4	0.10	5.63	24.20
Rh^{105}	Ar	281.8	199.5	0.145	7.02	26.62
Pd^{112}	H_2	176.4	95.5	0.23	0.53	12.74
Pd^{112}	He	336.6	262.8	0.12	1.33	14.97
Pd^{112}	Ne	268.3	286.1	0.10	6.78	23.04
Pd^{112}	Ar	243.7	181.4	0.145	9.18	30.80
Cd^{115}	H_2	161.2	90.2	0.23	0.54	13.10
Cd^{115}	He	308.0	249.0	0.12	1.44	18.14
Cd^{115}	Ne	246.8	269.0	0.10	7.46	41.47
Cd^{115}	Ar	225.1	174.9	0.145	10.01	39.56
Te^{132}	H_2	110.1	72.8	0.22	0.78	12.39
Te^{132}	He	211.2	202.1	0.12	2.23	16.72
Te^{132}	Ne	172.6	218.1	0.09	11.61	34.57
Te^{132}	Ar	160.1	148.0	0.13	16.28	40.57
Ce^{143}	H_2	80.2	59.2	0.22	1.02	11.08
Ce^{143}	He	154.2	160.7	0.12	3.23	14.74
Ce^{143}	Ne	127.6	175.7	0.09	16.02	36.00
Ce^{143}	Ar	119.6	122.3	0.13	22.80	59.90
Sm^{153}	H_2	59.8	51.5	0.22	1.16	12.81
Sm^{153}	He	115.2	141.1	0.11	3.58	26.01
Sm^{153}	Ne	96.2	151.5	0.09	19.39	34.57
Sm^{153}	Ar	90.9	108.0	0.13	26.44	39.18

where a_0 is the Bohr radius ($\hbar^2/me^2$), and γ is given by

$$\gamma = 4A_1A_2/(A_1+A_2)^2 . \tag{24}$$

It is convenient to define a factor f_{LSS}:

$$f_{\mathrm{LSS}} = \pi a^2 N . \tag{25}$$

This factor has the convenient property that

$$\rho_L = \langle R\rangle (f_{\mathrm{LSS}})(\gamma) . \tag{26}$$

The stopping power due to electronic processes is given by

$$\left(\frac{\partial \epsilon}{\partial x}\right)_e = k\epsilon^{1/2} , \tag{27}$$

where

$$k \cong \xi_e \frac{0.0793 Z_1^{2/3} Z_2^{1/2} (A_1+A_2)^{3/2}}{(Z_1^{2/3}+Z_2^{2/3})^{3/4} A_1^{3/2} A_2^{1/2}} , \tag{28}$$

and ξ_e can be taken to be approximately $Z_1^{1/6}$. The total stopping power is given by the sum of the electronic part and the ion-atom part, $(\partial\epsilon/\partial x)_n$,

$$\frac{\partial \epsilon}{\partial x} = k\epsilon^{1/2} + \left(\frac{\partial \epsilon}{\partial x}\right)_n . \tag{29}$$

Note that the electronic stopping power is taken as proportional to velocity and that k is defined as independent of energy in the LSS theory. If one uses range data to fix empirically the value of k, any energy dependence of k can be clearly noted.[27] LSS point out that empirical values of k may be more accurate than those from Eq. (28).[17]

In the present work, the theory of LSS[17] has been used to assist in the separation of fission-produced straggling ρ_s from measured straggling. In short, the theory predicts that ρ_s should increase with the mass of the stopper. Therefore, a plot is made of the measured values of the range straggling versus the theoretical values for the stopping straggling only. From the intercept one obtains ρ_f, and from the slope, ρ_s. This analysis is very similar to that of Refs. 4 and 6, but the more recent theory of LSS is used to calculate theoretical values of ρ_s.

In order to calculate ρ_s from the theory of LSS[17] it is first necessary to get the best values for k. These values were taken from the mean range measurements. The calculated values for ϵ, and ρ_L are summarized in Table VI for each product and stopper combination. The reduced range ρ_L is plotted vs ϵ in Fig. 4. Contour lines of equal k taken from the LSS paper[17] are superimposed. By interpolation an empirical k parameter for each point was taken from this graph. These em-

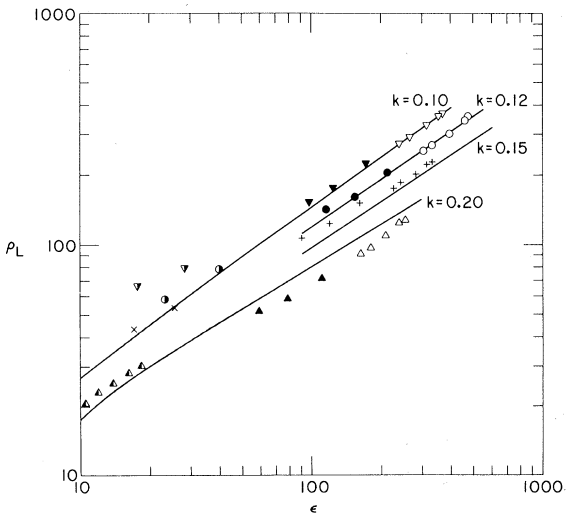

FIG. 4. Range measurements in the reduced coordinate ρ_L versus reduced energy ϵ. The different symbols are for the different stopping gases: △, H_2; ▽, Ne; ○, He; +, Ar. Heavy fission products, closed points; light fission products, open points. Contour lines of constant k have been superimposed from Ref. 17. Data from Ref. 15 on stopping of Dy ions have been added: ▲, H_2; ▼, Ne; ◑, He; ×, Ar.

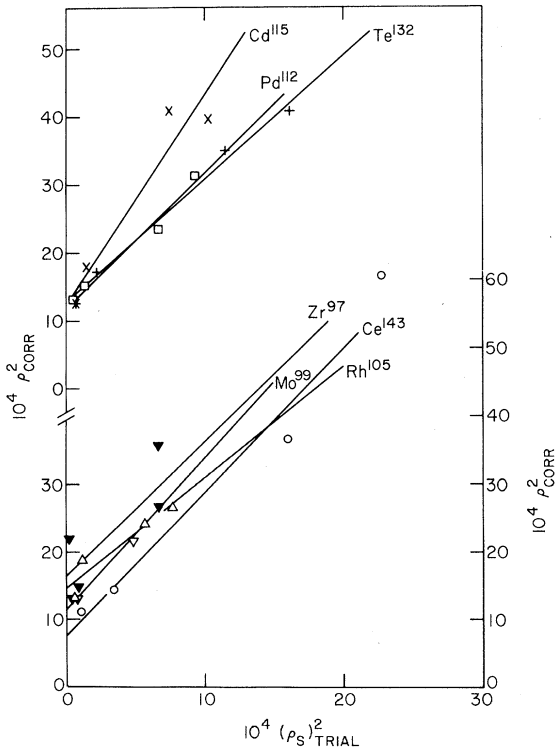

FIG. 5. The square of the total straggling parameter ρ^2_{corr} vs trial values $(\rho_s)^2_{trial}$. Right-hand ordinate: ○, Ce^{143}; ▽, Mo^{99}; △, Rh^{105}; ▼, Zr^{97}. Left-hand ordinate □, Pd^{112}; +, Te^{132}; ×, Cd^{115}.

TABLE VII. Fission-produced straggling parameters.

Observed product	Slope [a]	ρ_f
Zr^{97}	2.28	0.040
Mo^{99}	2.16	0.034
Rh^{105}	1.58	0.039
Pd^{112}	1.93	0.034
Cd^{115}	3.07	0.036
Te^{132}	1.84	0.035
Ce^{143}	2.09	0.027

[a] The slope is that shown in Fig. 5 where ρ^2_{corr} is plotted versus $(\rho^2_s)_{trial}$. The theory of Ref. 17 predicts a slope of unity.

pirical values of k from the range values are also given in Table VI; they in turn were used to estimate a "trial" value of the stopping-produced range variance[28] from the LSS theory $(\Delta\rho_L/\gamma)^2$. Then a trial value of the square of the stopping straggling parameter can be determined, since

$$\left(\frac{\Delta\rho_L}{\rho_L}\right)^2_{trial} = \frac{\Delta\rho_L^2}{\gamma}\,\frac{1}{\gamma f^2_{LSS}\langle R\rangle^2} = (\rho_s)^2_{trial}\,. \tag{30}$$

These values are also in Table VI, along with the empirical values of k from which they have been determined.

With these trial values of the stopping straggling parameter, one can separate the fission-produced straggling from the stopping-produced straggling. The relation between the two contributions to the experimental parameters is expected to be

$$\rho^2_{corr} = \left(\frac{\Delta\rho_L}{\rho_L}\right)^2_{meas} = \rho_s^2 + \rho_f^2 \tag{31}$$

$$= \rho^2_{corr}\left(\frac{\Delta\rho_L}{\rho_L}\right)^2_{trial} + \rho_f^2\,. \tag{32}$$

Hence if the trial values are correct, ρ^2_{corr} will be a linear function of $(\rho_s)^2_{trial}$ for a single product stopped in various gases. If $(\rho_s)^2_{trial}$ is not absolutely correct but gives the correct dependency on stopping gas, a plot of ρ^2_{corr} vs $(\rho_s)^2_{trial}$ should still yield a straight line. The intercept of this straight line should be the square of the fission-produced straggling, and the slope should be unity if the LSS theory is perfect. Such a plot is shown in Fig. 5. The slopes and the straggling parameters from fission alone ρ_f are listed in Table VII. (The results for Sm^{153} were excluded because of the low intensity of the observed γ rays as mentioned in the experimental section.) The slopes of the lines are all greater than unity; this indicates a weakness in the theoretical framework that is being used. This difficulty is probably not serious for the determination of ρ_f, because the contribution from stopping appears to be so small for the light gases H_2 and He.

TABLE VIII. Experimental stopping straggling parameters ρ_s compared with those from stopping theory $(\rho_s)_{trial}$.

Observed product	Stopping gas	ϵ	ρ_s	$(\rho_s)_{trial}$
Zr^{97}	Ne	368.3	0.023	0.022
Zr^{97}	Ar	327.7	0.044	0.026
Mo^{99}	Ne	352.3	0.030	0.022
Mo^{99}	Ar	314.4	0.040	0.026
Rh^{105}	Ne	313.2	0.031	0.024
Rh^{105}	Ar	281.8	0.034	0.028
Pd^{112}	Ne	268.3	0.034	0.026
Pd^{112}	Ar	243.7	0.044	0.030
Cd^{115}	Ne	246.8	0.053	0.027
Cd^{115}	Ar	225.1	0.052	0.032
Te^{132}	Ne	172.6	0.048	0.034
Te^{132}	Ar	160.1	0.054	0.040
Ce^{143}	Ne	127.6	0.054	0.040
Ce^{143}	Ar	119.6	0.073	0.048

The stopping straggling parameters that have been determined for Ne and Ar from Eq. (32) can be compared with the theory in a more direct way. In Table VIII the values of ρ_s are compared directly with the values of $(\rho_s)_{trial}$ from the theory. On the average, the measured values are about 35% larger than the theoretical values – a difference that is not very large for a theory developed from first principles. The difference is more visible in Fig. 5 because the quantities are all squared; it is reflected in the slope values of ≈ 2 rather than unity (see Table VII).

A measured value of the stopping straggling can also be used to determine a value of k, the elec-

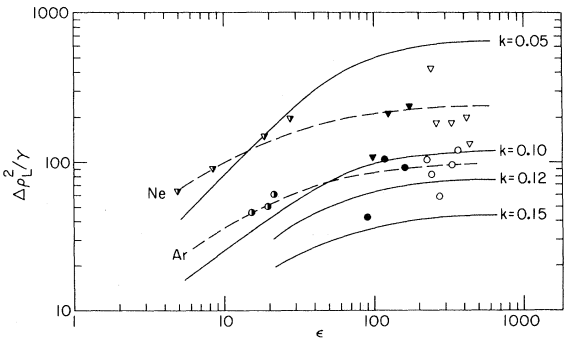

FIG. 6. The experimentally determined stopping straggling in reduced coordinates $(\Delta\rho_L^2/\gamma)$ versus reduced energy ϵ. ▽, Ne as a stopper; ○, Ar as a stopper. Open points are light fission products, closed points are heavy fission products, half-closed points are Dy^{149} from Ref. 14. Lines are contours of constant k from Ref. 17.

TABLE IX. Comparison of empirical values of k with theoretical values.

	ϵ	k from $\langle R \rangle$	k from ρ_s	k from LSS	ϵ	k from $\langle R \rangle$	k from ρ_s	k from LSS
		H_2				He		
Light fragments	160–250	0.22–0.23		0.13	307–474	0.13–0.12		0.10
Heavy fragments	50–110	0.21–0.22		0.14	115–211	0.11–0.12		0.11
Dy [a]	5–40	0.14–0.17		0.15	7–30	0.05–0.09		0.11
		Ne				Ar		
Light fragments	246–368	0.10	0.05–0.095	0.11	225–328	0.145	0.14–0.11	0.12
Heavy fragments	96–172	0.09	0.08–0.09	0.11	90–160	0.13	0.14–0.10	0.11
Dy [a]	5–27	0.04–0.06	0.04–0.05	0.11	6–22	0.07–0.1	0.25–0.095	0.11

[a] The values of k for Dy were taken from Ref. 15. They increase with energy over the span shown.

tronic stopping parameter. For this purpose each measurement has been transformed back into the appropriate variable $\Delta\rho_L^2/\gamma$ and plotted versus ϵ in Fig. 6. The intermediate parameters for this computation are listed in Table VIII. A set of values of k can be taken from this figure. They are of interest also, since the stopping straggling should be quite sensitive to the parameter k. These k values empirically determined from the straggling are completely independent of those from the mean ranges.

In Table IX the empirical values of k from both the stopping straggling and the mean range are summarized, together with the theoretical values. These values should all agree, of course. There is in general a reasonable agreement between the empirical values from the mean range and the stopping straggling. However, there is considerable disagreement between the theoretical k parameter and the empirical values. Also it is evident from the k values in Table IX, that there is a definite trend toward higher values of k with increasing ϵ. This trend was noticed by Gilat and Alexander[15] for Dy nuclei at much lower energies ($\epsilon = 5$ to 30). It evidently continues, as the k values determined in the present work are all larger than those determined for the low-energy Dy recoils. The experimental methods of this work and Ref. 19 are quite similar, as both used gas stopping with electrostatic collection. Gilat and Alexander[15] ascribe the trend of increasing values of k with ϵ to an electronic stopping power that is not strictly proportional to $\epsilon^{1/2}$. The results of this work are consistent with this proposal, and with the trends of the former work.[15]

V. SUMMARY

Measured values of the average range and range straggling for fission products are compared with the stopping theory of LSS. The trends of the data follow the theoretical predictions, but the detailed behavior of the electronic stopping is not very well accounted for. The average ranges in H_2 are about $\frac{1}{2}$ of the predicted values. The straggling parameters are all about 35% larger than those predicted. The experimental results can be used to fix empirically a set of electronic stopping parameters that unify the average ranges and the range stragglings.

ACKNOWLEDGMENTS

We are grateful to D. Burgess and A. Sanders for help with the electronic and the computing equipment. The hospitality of Brookhaven National Laboratory and a NASA Traineeship (1967–1970) is gratefully acknowledged by M. P. We are also grateful to M. L. Perlman and J. B. Cumming for many helpful discussions, and for reading the early drafts of this manuscript.

*Research sponsored by the U. S. Atomic Energy Commission.

[1] M. Pickering and J. M. Alexander, following paper, Phys. Rev. C 6, 343 (1972).

[2] S. Katcoff, J. A. Miskel, and C. W. Stanley, Phys. Rev. 74, 631 (1948).

[3] K. V. Marsh and J. A. Miskel, J. Inorg. Nucl. Chem. 21, 15 (1961).

[4]W. M. Good and E. O. Wollan, Phys. Rev. 101, 249 (1956).
[5]J. M. Alexander and M. F. Gazdik, Phys. Rev. 120, 874 (1960).
[6]K. A. Petrzhak, Yu. G. Petrov, and E. A. Shlyamin, Zh. Eksperim. i Teor. Fiz. 38, 1723 (1960) [transl.: Soviet Phys.-JETP 11, 1244 (1960)].
[7]J. B. Niday, Phys. Rev. 121, 1471 (1961).
[8]J. M. Alexander, M. F. Gazdik, A. R. Trips, S. Wasif, Phys. Rev. 129, 2659 (1963).
[9]N. K. Aras, M. P. Menon, and G. E. Gordon, Nucl. Phys. 69, 337 (1965).
[10]J. B. Cumming and V. P. Crespo, Phys. Rev. 161, 287 (1967).
[11]O. Birgül, I. Ölmez, and N. K. Aras, to be published.
[12]E. W. Valyocsik, UCRL Report No. UCRL 8855, 1959 (unpublished).
[13]L. Bryde, N. O. Lassen, and N. O. Roy Poulsen, Kgl. Danske Videnskab. Selskab, Mat.-Fys. Medd. 33, No. 8 (1962).
[14]J. M. Alexander, J. Gilat, and D. H. Sisson, Phys. Rev. 136, B1289 (1964).
[15]J. Gilat and J. M. Alexander, Phys. Rev. 136, B1238 (1964).
[16]N. T. Porile and I. Fujiwara, Phys. Rev. 176, 1166 (1968).
[17]J. Lindhard, M. Scharff, and H. E. Schiøtt, Kgl. Danske Videnskab. Selskab, Mat.-Fys. Medd. 33, No. 14 (1963).
[18]W. Nervik, Phys. Rev. 119, 1685 (1960).
[19]C. M. Lederer, J. M. Hollander, and I. Perlman, *Table of Isotopes* (Wiley, New York, 1967), 6th ed.
[20]N. A. Fuchs, *The Mechanics of Aerosols* (Pergamon, New York, 1964).
[21]Equation (7) is true only for singly charged ions. If the ions have greater than unit charges they will be collected more rapidly, and the diffusion correction will be smaller.
[22]W. Jost, *Diffusion in Solids, Liquids, and Gases* (Academic, New York, 1952).
[23]H. Cramer, *Mathematical Methods of Statistics* (Princeton U. P., Princeton, N. J., 1951), p. 361.
[24]A. C. Wahl, A. E. Norris, R. A. Rouse, and J. C. Williams, in *Proceedings of the Second International Atomic Energy Agency Conference on the Physics and Chemistry of Fission, Vienna, Austria, 1969* (International Atomic Energy Agency, Vienna, Austria, 1969), p. 813.
[25]C. D. Coryell, M. Kaplan, and R. D. Fink, Can. J. Chem. 39, 646 (1961).
[26]E. Cheifetz, J. B. Wilhelmy, R. C. Jared, and S. G. Thompson, UCRL Report No. UCRL-20498 (unpublished).
[27]For the purposes of argument the heavy and light fission fragments have been grouped, and so correlations of Z, A, and ν with k have been neglected. One of the purposes of the reduced variables ρ_L and ϵ is to eliminate the effect of Z and A.
[28]Figure 7 in LSS gives a plot of the stopping variance $(\Delta\rho_L)^2/\gamma$ vs ϵ with contour lines of constant k.

PHYSICAL REVIEW C VOLUME 6, NUMBER 1 JULY 1972

Range Measurements of Fission Products. II. Kinetic Energy Deficit and Width of the Energy Distributions*

Miles Pickering and John M. Alexander
Department of Chemistry, State University of New York, Stony Brook, New York 11790
(Received 6 December 1971)

Range measurements of fission products (Zr^{97}, Mo^{99}, Rh^{105}, Pd^{112}, In^{115}, Te^{132}, Ce^{143}) in gases have been compared with the range-energy tables of Northcliffe and Schilling. A re-evaluation of the kinetic energy deficit for symmetric fission has been made, using a modification of these range-energy relationships. Experimental measurements of range distributions of fission fragments stopped in gases have been used to determine the width of the kinetic energy distributions as a function of product mass. The values obtained are compared with those from other workers.

I. INTRODUCTION

This paper is the second of two dealing with the ranges of fission fragments in gases.[1] In this paper the measured average ranges for eight different fission products are compared with range-energy tables of Northcliffe and Schilling.[2] The ratio of measured to tabulated ranges depends only slightly on the mass of the fragment. This has enabled us to convert previously measured ranges[3-12] for low-yield fission products into energies. Ranges for species whose energies are well known from counter measurements[13-15] have been used to normalize the range-energy relationships. These range-energy curves in turn are then used to determine energies of products in near-symmetric fission from radiochemical range data. For these low-yield products only radiochemical